

# Journal of Materials Chemistry C

Accepted Manuscript



This is an *Accepted Manuscript*, which has been through the Royal Society of Chemistry peer review process and has been accepted for publication.

*Accepted Manuscripts* are published online shortly after acceptance, before technical editing, formatting and proof reading. Using this free service, authors can make their results available to the community, in citable form, before we publish the edited article. We will replace this *Accepted Manuscript* with the edited and formatted *Advance Article* as soon as it is available.

You can find more information about *Accepted Manuscripts* in the [Information for Authors](#).

Please note that technical editing may introduce minor changes to the text and/or graphics, which may alter content. The journal's standard [Terms & Conditions](#) and the [Ethical guidelines](#) still apply. In no event shall the Royal Society of Chemistry be held responsible for any errors or omissions in this *Accepted Manuscript* or any consequences arising from the use of any information it contains.

## ARTICLE

# Red Emissive Organic Light-Emitting Diodes based on Codeposited Inexpensive Cu<sup>I</sup> Complex<sup>†</sup>

Cite this: DOI: 10.1039/x0xx00000x

Tianchi Ni,<sup>a</sup> Xiaochen Liu,<sup>a</sup> Tao Zhang,<sup>b</sup> Hongliang Bao,<sup>c</sup> Ge Zhan,<sup>a</sup> Nan Jiang,<sup>b</sup> Jianqiang Wang,<sup>c\*</sup> Zhiwei Liu,<sup>a\*</sup> Zuqiang Bian,<sup>a</sup> Zhenghong Lu<sup>b</sup> and Chunhui Huang<sup>a</sup>

Received 00th January 2012,  
Accepted 00th January 2012

DOI: 10.1039/x0xx00000x

www.rsc.org/

Inexpensive materials made of abundant natural resources such as Cu<sup>I</sup> complexes is essential to sustain development of organic light emitting diodes (OLEDs) technology for mass market applications such as solid-state illumination. Cu<sup>I</sup> complexes, however, most are neither soluble nor stable toward sublimation, which is a road block for the development of efficient Cu<sup>I</sup> complex based OLEDs using traditional method of synthesis, sublimation and vacuum evaporation. In this work, two isoquinolyl carbazole (CIQ) compounds were synthesized to codeposition with copper iodide (CuI) to form red emissive dimeric Cu<sup>I</sup> complex doped film *in situ*, which could be utilized directly as the emissive layer (EML) in OLEDs. After a systematically study of the two compounds and their codeposited CuI:CIQ films, as well as optimizing CuI doping concentration, it is found that red OLEDs can be achieved, showing maximum emission band, external quantum efficiency (EQE), luminance of 643 nm, 3.5%, 3290 cd m<sup>-2</sup> for DCIQ, and 635 nm, 3.6%, 853 cd m<sup>-2</sup> for DCDPIQ, respectively.

## Introduction

Organic light emitting diodes (OLEDs) have been successfully commercialized in niche market such as smart phone displays and 3D curved televisions, and are now under intense research for other applications such as solid-state lightings.<sup>1-11</sup> Phosphorescent OLEDs (PHOLEDs), which promise an internal quantum efficiency of up to 100%, have been considered as the ultimate energy-saving technology.<sup>10,12-14</sup> So far the best performing PHOLEDs are based on noble transition metal (i.e. iridium and platinum) complexes.<sup>15,16</sup> Unfortunately, iridium and platinum are low in natural abundance, which presents a significant barrier to commercialization. Therefore, there have been significant efforts devoted to developing more cost-effective solutions to achieve high quantum efficiency in OLEDs.<sup>17</sup>

Cu<sup>I</sup> complexes are considered as a good alternative emitter for OLEDs, considering their low cost and potential high performance.<sup>18-20</sup> The earliest Cu<sup>I</sup> complex applied in OLED is a tetranuclear Cu<sup>I</sup> compound, [Cu<sub>4</sub>(C≡CPh)<sub>4</sub>L<sub>2</sub>] [L = 1,8-bis(diphenylphosphino)-3,6-dioxaoctane].<sup>21</sup> Although the compound showed a green phosphorescence at 520 nm with photoluminescence quantum yield (PLQY) of 42%, the compound is non-volatile, and a solution processed OLED showed external quantum efficiency (EQE) of only 0.1%. As time goes on, the Cu<sup>I</sup> complex based OLEDs, especially the green emissive ones, are moving forward step by step.<sup>22-33</sup> For example, researchers have fabricated OLEDs with heteroleptic diimine/diphosphine complexes [Cu(N<sup>^</sup>N)(P<sup>^</sup>P)]<sup>+</sup>. It has been shown that they can be profitably used as electrophosphorescent emitters and provide EQE around

3.6%.<sup>19,23</sup> Recently, Peters *et al.* have obtained a sublimable and highly emissive Cu<sup>I</sup> complex (PLQY = 57%) with tightly bound chelate ligand that can create a rigid environment around the copper center and hence fabricated an efficient green OLED with maximum EQE of 16.1%.<sup>28</sup> Osawa *et al.* have fabricated even more efficient green OLED with a maximum EQE of 21.3%, by using a sublimable and simple three-coordinate Cu<sup>I</sup> complex as the emitter.<sup>29</sup>

Though great improvement has been made in green emissive OLEDs, the development of the other two primary colours, red and blue emissive Cu<sup>I</sup> complex based OLEDs are rare.<sup>24,27,28,34,35</sup> Considering that a long time has been passed since the first example of Cu<sup>I</sup> complex based OLED demonstrated in 1998, the development of Cu<sup>I</sup> complex based OLEDs is very slow, especially comparing with iridium complex based OLEDs. The main reason is that most Cu<sup>I</sup> complexes are unstable during sublimation and hence not amenable to the vacuum deposition methods typically used to fabricate OLEDs.

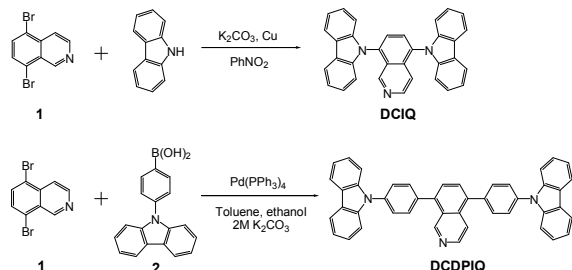
By using a codeposition method, which involves codeposition of copper iodide (CuI) and pyridine-coordinating ligand/host compound to form a halogen-bridged dinuclear Cu<sup>I</sup> complex Cu<sub>2</sub>(μ-I)<sub>2</sub>L<sub>4</sub> (L stands for pyridine-coordinating ligand/host compound) doped emissive layer (EML) *in situ*,<sup>30</sup> we have demonstrated a green emissive OLED with an EQE up to 15.7% at 100 cd/m<sup>2</sup>, which is comparable to that of iridium complex OLEDs.<sup>36</sup> The codeposition method has been proved to be useful to fabricate green emissive Cu<sup>I</sup> complex based OLEDs, next comes the question of how to tune the emission colour of the *in situ* synthesized Cu<sup>I</sup> complex to red or blue, the other two primary colours and hence fabricate colourful OLEDs.

According to literatures,<sup>26,37,38</sup> the electron density in the highest occupied molecular orbitals (HOMOs) of a halogen-bridged dinuclear Cu<sup>I</sup> complex Cu<sub>2</sub>(μ-I)<sub>2</sub>L<sub>4</sub> is distributed over the copper and iodine atoms, while that in the lowest unoccupied molecular orbitals (LUMOs) is localized on the ligands. Thus, the emission colour of the *in situ* formed Cu<sup>I</sup> complex could be tuned by varying the electronic structure of the codeposited ligand. Moreover, the codeposited ligand in this case serves a dual role as both a ligand for forming the emissive complex and as a host matrix for the formed emitter, thus the ligand should also be carefully designed to ensure that it is both a good ligand for Cu<sup>I</sup> coordination and a good host matrix for the *in situ* formed Cu<sup>I</sup> complex.

Following aforementioned considerations, two isoquinolyl carbazole (CIQ) compounds 9-(8-(carbazol-9-yl)isoquinolin-5-yl)-carbazole (DCIQ) and 9-(4-(5-(4-(carbazol-9-yl)phenyl)isoquinolin-8-yl)phenyl)-carbazole (DCDPIQ) were designed and synthesized. The isoquinolyl coordinating unit is mainly designed to realize a red-shifted emission colour of the *in situ* formed Cu<sup>I</sup> complex comparing to that of pyridinyl.<sup>30,36</sup> The electrical properties of the two compounds were tuned by varying the central arylene. After a systematically study of the two compounds and their codeposited CuI:CIQ films, it is found that the codeposited CuI:DCIQ and CuI:DCDPIQ films showed red emission with maximum wavelength around 631 and 617 nm, respectively. By adopting the codeposited CuI:DCIQ or CuI:DCDPIQ film as the EML, red OLEDs with maximum emission band, EQE, luminance of 643 nm, 3.5%, 3290 cd m<sup>-2</sup>, and 635 nm, 3.6%, 853 cd m<sup>-2</sup>, respectively, were obtained.

## Results and discussion

### Synthesis and characterization



Scheme 1. Synthetic routes to DCIQ and DCDPIQ.

The synthetic routes and chemical structures of DCIQ and DCDPIQ are depicted in Scheme 1. The compound DCIQ was synthesized through a Ullman coupling reaction of 5,8-dibromoisoquinoline<sup>39</sup> and carbazole, while the compound DCDPIQ was synthesized through a Suzuki coupling reaction of 5,8-dibromoisoquinoline and 4-(carbazol-9-yl)phenylboronic acid<sup>40</sup>. After purified by flash column chromatography on silica gel, the compound was subsequently underwent twice thermal gradient sublimations. The characterization of the two compounds was established on the basis of <sup>1</sup>H and <sup>13</sup>C NMR spectroscopy, mass spectrometry, and elemental analysis. Details are presented in the Experimental Section.

### Photophysical properties

Fig. 1 shows the electronic absorption and fluorescence spectra in CH<sub>2</sub>Cl<sub>2</sub> at 298K, and phosphorescence in 2-MeTHF

at 77K of the compounds DCIQ and DCDPIQ. An absorption peak at around 240 nm and a shoulder at 260 nm can be attributed to π-π\* and n-π\* transitions of central arylene, respectively. Absorption peaks around 290 and 340 nm can be attributed to π-π\* transitions of the carbazole chromophore. Absorbance at wavelengths longer than 350 nm increases with carbazole connected directly to the isoquinolyl. This can be attributed to strong electron affinity of isoquinolyl and intramolecular charge transfer formed between carbazole and isoquinolyl.

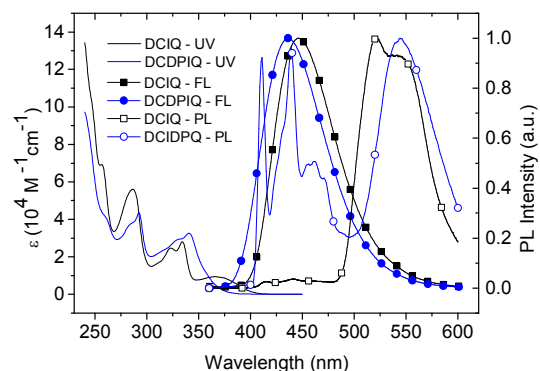


Fig. 1. UV-vis absorption, fluorescence (FL), and phosphorescence (PL) spectra of DCIQ and DCDPIQ.

The two compounds showed strong blue emission in CH<sub>2</sub>Cl<sub>2</sub>, with maximum emission bands at 446 and 436 nm (Fig. 1, Table 1), PLQY of 0.36 and 0.85, and the Commission Internationale de L'Eclairage (CIE) coordinates of (0.15, 0.10) and (0.15, 0.08) for DCIQ and DCDPIQ, respectively. Based on density functional theory (DFT) calculation, the HOMOs of the two compounds are mainly located at the carbazole unit. In contrast, the LUMOs are mainly distributed on the central arylene (Fig. S1, Table S1). Herein, the observed emission could be attributed to an intramolecular charge transfer between carbazole and isoquinolyl.

Besides serving as a ligand, the compound is also expected to be a host matrix for the *in situ* formed Cu<sup>I</sup> complex. Therefore, the triplet energy level (E<sub>T</sub>) difference between the compound and its *in situ* synthesized Cu<sup>I</sup> complex is a very important parameter to estimate the energy transfer status between them. The E<sub>T</sub> data are deduced from the low temperature PL spectrum for the compound, and of room temperature PL spectrum for the Cu<sup>I</sup> complex, which will be discussed herein and hereafter, respectively. Based on the low temperature PL spectra of DCIQ and DCDPIQ in 2-MeTHF solution at 77 K (Fig. 1), the T<sub>1</sub> energy levels for DCIQ and DCDPIQ are 521 nm (2.4 eV) and 545 nm (2.3 eV), respectively. It should be noted that a higher E<sub>T</sub> of T<sub>2</sub> were also observed both for DCIQ and DCDPIQ, having value of 415 nm (3.0 eV) and 411 nm (3.0 eV), respectively. The data is consistent with our DFT studies on DCIQ and DCDPIQ (Table S1) by calculating the difference of their ground state (S<sub>0</sub>) and triplet excited states (T<sub>1</sub> and T<sub>2</sub>) energies at the B3LYP/6-31G(d) and B3LYP/6-311+G(d,p) levels, respectively.

Solid state emission is essential for practical applications of luminescent materials. Hence, we examined the emission of the two compounds in the solid state at room temperature and 77 K with a fluorescence and phosphorescence model, respectively (Fig. S2). Similar to those observed in solutions, the two compounds showed strong blue emission with maximum emission bands at 442 and 438 nm, PLQY of 0.30 and 0.74, and CIE coordinates of (0.17, 0.14) and (0.16, 0.11) for DCIQ and DCDPIQ at room temperature, respectively. The maximum emission wavelengths are similar to those observed in the solution, indicating a weak intermolecular interaction. When examined at 77 K with a phosphorescence model, both  $T_1$  and  $T_2$  were found for the two compounds, which is consistent with the phenomenon observed in solution.

**Table 1.** The photophysical, electrochemical, and thermal properties of DCIQ and DCDPIQ.

Compd.	$E_g$ [eV] <sup>(a)</sup>	$\lambda_{em}$ [nm] <sup>(b)</sup>	$\lambda_{em}$ [nm] <sup>(c)</sup>	$E_T$ [eV] <sup>(d)</sup>	HOMO/LUMO [eV] <sup>(e)</sup>	$T_g/T_s$ [°C] <sup>(f)</sup>
DCIQ	3.1	446	442	2.4	6.0/2.9	118/405
DCDPIQ	3.3	436	438	2.3	5.8/2.5	144/511

<sup>(a)</sup>Calculated from the limit of absorption spectrum; <sup>(b)</sup>Measured in  $\text{CH}_2\text{Cl}_2$  ( $10^{-5}$  M); <sup>(c)</sup>Measured in solid state; <sup>(d)</sup>Deduced from low temperature PL spectrum; <sup>(e)</sup>HOMO was determined from the oxidation potential, LUMO was deduced from the formula  $E_g = \text{LUMO} - \text{HOMO}$ ; <sup>(f)</sup>Determined by TGA and DSC measurements.

### Thermal properties

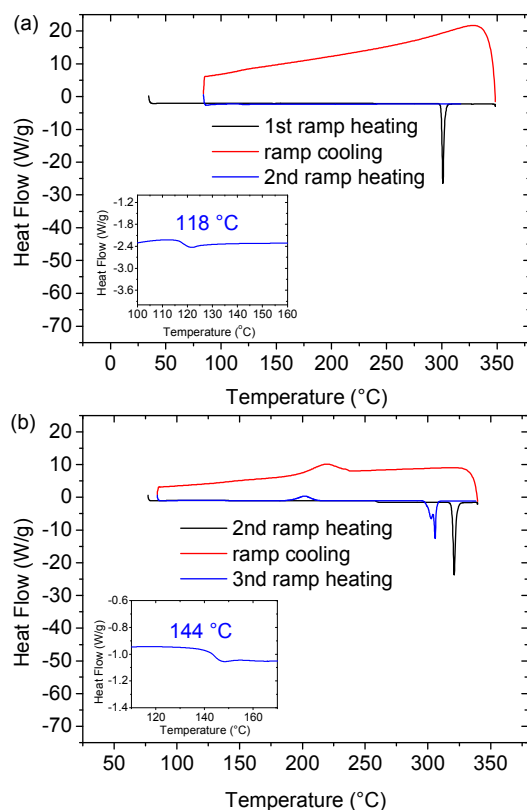


**Fig. 2.** DSC thermograms of (a) DCIQ and (b) DCDPIQ recorded at a heating rate of  $15\text{ °C min}^{-1}$ .

The thermal properties of the two compounds were investigated by thermogravimetric analysis (TGA, Fig. S3) and

differential scanning calorimetry (DSC, Fig. 2). TGA measurement reveals their high sublimation temperatures ( $T_s$ , corresponding to 5% weight loss) of 405 and 511 °C for DCIQ and DCDPIQ, respectively, which are higher than 373 °C of 4,4'-N,N'-dicarbazole-biphenyl (CBP, a widely used host material in OLEDs). During the DSC measurement, it is found that the glass-transition temperatures ( $T_g$ ) are 118 and 144 °C for DCIQ and DCDPIQ, respectively, which are significantly higher than 62 °C of CBP<sup>41</sup> and 95 °C of 1,4-bis[(1-naphthylphenyl)amino]biphenyl (NPB)<sup>42</sup>. The high  $T_g$  of our compounds may guarantee the stability of the corresponding OLEDs, since it has been reported that the surface temperature at the site of the electrical short is as high as 86 °C and the temperature inside actual OLEDs can be even higher.<sup>43</sup>

### Electrochemical properties

Cyclic voltammetry was employed to investigate the electrochemical properties of the two compounds and hence to estimate their HOMO/LUMO energy levels. In particular, the oxidation process was investigated in  $\text{CH}_2\text{Cl}_2$  solution with ferrocene as an internal standard (Fig. 3). On the basis of the cyclic voltammetry curves, the oxidation potentials were observed to be 1.0 and 0.8 V, thus the HOMO energy levels were roughly estimated to be 6.0 and 5.8 eV by using an empirical formula ( $E_{\text{HOMO}} = -(1.4 \pm 0.1) \times (qV_{\text{CV}}) - (4.6 \pm 0.08)$  eV, where  $q$  is the electron charge and  $V_{\text{CV}}$  is the relative oxidation potential).<sup>44</sup> The LUMO energy levels were deduced from HOMO energy levels and optical band gaps (i.e.  $E_g$ ), which are 2.9 and 2.5 eV for DCIQ and DCDPIQ, respectively (Table 1). This implies that holes and electrons could be injected into the two compounds with small obstruction from CBP ( $E_{\text{HOMO}} = 6.1\text{ eV}$ <sup>36</sup>) and 1,3,5-tris(N-phenylbenzimidazole-2-yl) benzene (TPBi,  $E_{\text{LUMO}} = 2.8\text{ eV}$ <sup>36</sup>), respectively.

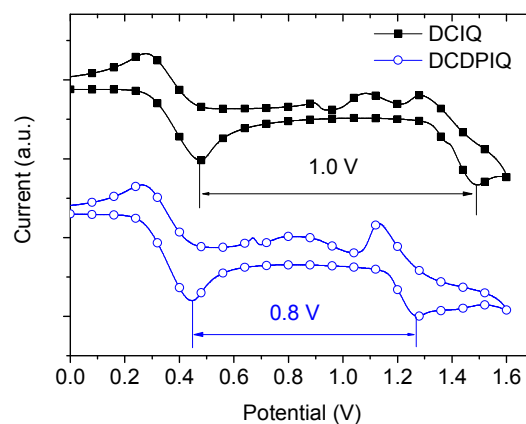


**Fig. 3.** Cyclic voltammogram of DCIQ and DCDPIQ using ferrocene as an internal standard.

### Photophysical Properties of Codeposited films

Fig. 4 shows the PL spectra of CIQ neat films and CuI:CIQ (CIQ = DCIQ and DCDPIQ) films made by codepositing CuI and CIQ from two separate heating sources in a vacuum chamber, where the CuI:CIQ molar ratio was 1:7. The CIQ

compound showed strong blue emission in thin film, with maximum emission bands at 438 and 428 nm, PLQY of 0.54 and 0.46, and CIE coordinates of (0.16, 0.10) and (0.16, 0.10) for DCIQ and DCDPIQ, respectively. While their codeposited CuI:CIQ films have dominated red emission with maximum emission bands at 631 and 617 nm, PLQY of 0.16 and 0.14, and CIE coordinates of (0.55, 0.36) and (0.46, 0.33) for CuI:DCIQ and CuI:DCDPIQ, respectively, which is differ markedly from the neat CIQ film, implying the formation of Cu<sup>I</sup> complexes and energy transfer between the un-complexed compound and its *in situ* synthesized Cu<sup>I</sup> complex.<sup>30,36</sup> By tuning the CuI:CIQ molar ratio from 1:7 to 1:1, 1:3, 1:5 or 1:9, it is found that the CuI:DCIQ film showed a PLQY in the range of 0.15-0.24, while the CuI:DCDPIQ film showed a lower PLQY in the range of 0.12-0.15 (Table S2). A redshift (14 nm) was found in the maximum PL wavelength of the codeposited CuI:CIQ films when the CIQ ligand was varied from DCDPIQ to DCIQ. Theoretically, the electron density in the HOMOs of the codeposited Cu<sup>I</sup> complex is distributed over the copper and iodine atoms, which are almost the same in the two cases, while that in the LUMOs is localized on the ligands.<sup>26,37,38</sup> Thus, the difference in emission colour of the *in situ* formed Cu<sup>I</sup> complex should be arisen mainly from the electronic structure of the codeposited ligand.

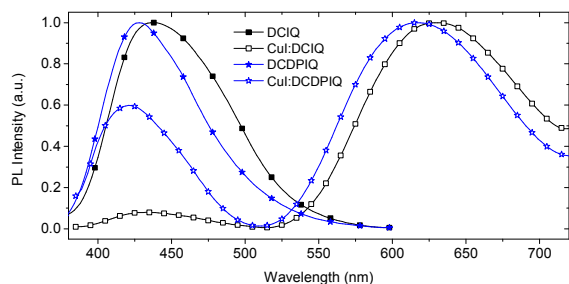


Fig. 4. PL spectra of the neat CIQ (CIQ = DCIQ or DCDPIQ) films and codeposited CuI:CIQ films with CuI:CIQ molar ratio of 1:7.

According to aforementioned low temperature PL study and DFT calculation, the  $E_T$  are around 2.4 and 2.3 eV for DCIQ and DCDPIQ, respectively. While based on the PL spectra of the codeposited CuI:CIQ films, the energy levels of the *in situ* synthesized Cu<sup>I</sup> complexes are around 2.0 eV (631 nm) and 2.0 eV (617 nm) for CuI:DCIQ and CuI:DCDPIQ, respectively. Since the triplet energies of the CIQ compounds are higher than their *in situ* synthesized Cu<sup>I</sup> complexes, energy transfer from the CIQ compound and its *in situ* synthesized Cu<sup>I</sup> complex could be guaranteed. As a result, both DCIQ and DCDPIQ may serve as good host matrix for their *in situ* synthesized Cu<sup>I</sup> complexes.

### Chemical Structure in the Codeposited Film

To illustrate the possible chemical structure of the *in situ* synthesized Cu<sup>I</sup> complex in film, a codeposited CuI:DCDPIQ film (molar ratio = 1:5) was measured by X-ray absorption fine structure (XAFS), including X-ray absorption near edge structure (XANES) and extended X-ray absorption fine

structure (EXAFS). Fig. 5 shows the XANES spectrum of the codeposited film, as well as those of Cu foil, Cu<sub>2</sub>O, CuO and CuBr<sub>2</sub> as references. The edge position of the film is shifted to high energy as compared with that of the Cu foil, indicating a Cu cation species. The pre-edge peak at about 8978 eV that corresponding to the  $1s \rightarrow 3d$  transition results from the  $d^9$  configuration of both CuO and CuBr<sub>2</sub>. In contrast, no pre-edge peak was observed in both Cu<sub>2</sub>O and the codeposited film, indicates a  $d^{10}$  configuration of Cu. Consequently, the presence of only monovalent Cu could be deduced in the sample.<sup>36,45</sup>

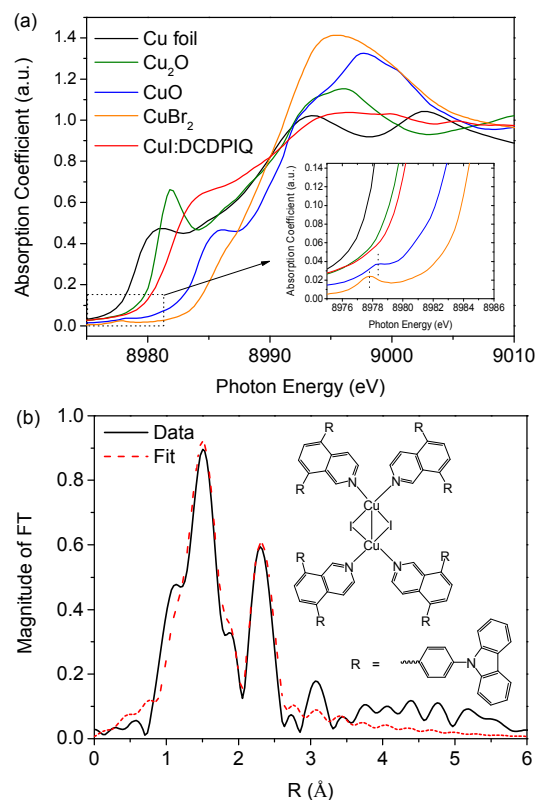


Fig. 5. (a) Cu *K*-edge XANES spectra of codeposited CuI:DCDPIQ film (CuI:DCDPIQ = 1:5) and Cu foil, Cu<sub>2</sub>O, CuO, CuBr<sub>2</sub> as references, insert: the magnification of the pre-edges for these XANES spectra. (b) Fourier transform of the codeposited CuI:DCDPIQ film (without phase shift corrected), data and fit waves are shown. Inset: Chemical structure of Cu<sub>2</sub>(μ-I)<sub>2</sub>(DCDPIQ)<sub>4</sub>.

Table 2. Fit parameters for the codeposited CuI:DCDPIQ film (CuI:DCDPIQ = 1:5).

Path	CN <sup>a)</sup>	R [Å] <sup>b)</sup>	$\sigma^2 \times 10^{-3} [\text{Å}^2]$ <sup>c)</sup>	$\Delta E_0$ (eV) <sup>d)</sup>	$S_0^2$
Cu-N	2.0	1.94 ± 0.01	3.1 ± 0.9	1.0	0.8
Cu-I	2.0	2.52 ± 0.02	8.1 ± 1.2	0.2	0.6
Cu-Cu	1.0	2.51 ± 0.04	12.0 ± 4.9	0.5	0.6

<sup>a)</sup>Coordination number; <sup>b)</sup>Distance between the Cu atom and surrounding N, I and Cu atoms; <sup>c)</sup>Mean square disorder; <sup>d)</sup>Inner potential shift.  $S_0^2$  is the amplitude decay factor.

Because the shape of XANES spectra is sensitive to the local geometric structure of absorption atoms, the dominant local geometric structure was determined by calculating the Cu *K*-edge XANES spectra for different structural model using FEFF8 code.<sup>46</sup> The calculated spectra of Cu<sub>2</sub>I<sub>2</sub>N<sub>4</sub> is most similar to experimental data of the codeposited CuI:DCDPIQ film, indicating the dominant structure of Cu<sub>2</sub>I<sub>2</sub>L<sub>4</sub> dimer (Fig.

S4). The structural parameters are further obtained by fitting the EXAFS data according to the structure of  $\text{Cu}_2\text{I}_2\text{L}_4$ . The Fourier transform of EXAFS fit parameters are listed in Fig. 5b and Table 2. There are three kinds of coordination structure including two Cu-N ( $1.94 \pm 0.01 \text{ \AA}$ ), two Cu-I ( $2.52 \pm 0.02 \text{ \AA}$ ), and one Cu-Cu ( $2.51 \pm 0.04 \text{ \AA}$ ) paths around the  $\text{Cu}^{\text{I}}$  center. Thus, the  $\text{Cu}^{\text{I}}$  species in the codeposited  $\text{CuI}:\text{DCDPIQ}$  films is most likely a dimeric complex  $\text{Cu}_2(\mu\text{-I})_2(\text{DCDPIQ})_4$  (Fig. 5b, insert).

### Electroluminescence Properties

To evaluate the codeposited  $\text{CuI}:\text{CIQ}$  films as EML, a series of OLEDs with a structure of  $\text{ITO}/\text{MoO}_3$  (1 nm)/  $\text{CBP}$  (35 nm)/  $\text{CuI}:\text{DCIQ}$  or  $\text{DCDPIQ}$  (20 nm)/  $\text{TPBi}$  (65 nm)/  $\text{LiF}$  (1 nm)/  $\text{Al}$  have been fabricated. The energy level diagram is shown in Fig. 6. The combination of  $\text{ITO}/\text{MoO}_3/\text{CBP}$  was used as the hole injection media since the thin  $\text{MoO}_3$  layer enables direct injection of holes into  $\text{CBP}$ , as well as excellent hole transport ability of  $\text{CBP}$ . The  $\text{TPBi}$  layer was used as the electron transport layer because of its proper LUMO energy level and good electron transport ability. Moreover, the triplet energies of  $\text{CBP}$  and  $\text{TPBi}$  are around 2.6 eV<sup>31,47</sup> which is higher than those of the *in situ* formed emitters  $\text{CuI}:\text{DCIQ}$  and  $\text{CuI}:\text{DCDPIQ}$ , resulting in an exciton confinement structure that beneficial for achieving high efficiency in OLEDs.<sup>31</sup>

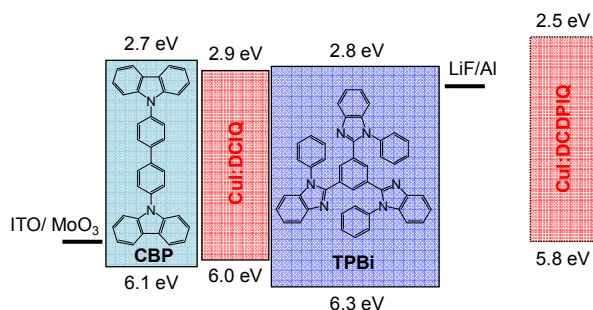


Fig. 6. The schematic device structure, chemical structure, and energy level diagrams of the molecules used in OLEDs.

Table 3. Performance of OLEDs 1-8.

Device	$V_{\text{on}}^{\text{a}}$ [V]	$L^{\text{b}}$ [ $\text{cd m}^{-2}$ ]	$\text{PE}^{\text{c}}$ [ $\text{lm W}^{-1}$ ]	$\text{CE}^{\text{c}}$ [ $\text{cd A}^{-1}$ ]	$\text{EQE}^{\text{c}}$ [%]	$\text{CIE}^{\text{d}}$
1	3.5	1632	1.9/0.8	2.1/1.4	1.7/1.1	(0.17, 0.16)
2	3.7	3290	3.8/2.6	4.6/4.6	3.5/3.5	(0.59, 0.39)
3	3.7	2421	2.9/1.9	3.4/3.5	2.9/2.9	(0.61, 0.39)
4	3.7	2350	2.7/1.8	3.1/3.3	2.7/2.9	(0.61, 0.38)
5	3.7	1743	1.7/1.0	1.9/1.6	2.0/1.7	(0.17, 0.13)
6	3.4	853	4.8/1.1	5.2/2.1	3.6/1.4	(0.58, 0.40)
7	3.4	800	4.5/1.1	5.0/2.1	3.5/1.4	(0.58, 0.40)
8	3.2	738	3.2/1.0	3.3/1.8	2.5/1.3	(0.59, 0.40)

<sup>a</sup> $V_{\text{on}}$  is the voltage required to reach a brightness of  $1 \text{ cd m}^{-2}$ ; <sup>b</sup>Luminance (L) recorded at 15 V; <sup>c</sup>Data for luminance at 1 and  $100 \text{ cd m}^{-2}$ , respectively; <sup>d</sup>Measured at a current of 50 mA.

To investigate the effect of  $\text{CuI}$  doping concentration on device performance, eight OLEDs with  $\text{CuI}$  mass doping concentrations of 0 wt% (devices 1 and 5), 1.0 wt% (devices 2 and 6), 2.0 wt% (devices 3 and 7), and 5.0 wt% (devices 4 and

8) were fabricated, where the ligand/host molecule for devices 1-4 is DCIQ, while that for devices 5-8 is DCDPIQ. Fig. 7 and 8 show the electroluminescence (EL) spectra, current density–voltage (CD-V), luminance–voltage (L-V), and external quantum efficiency–luminance (EQE-L) characteristics of these devices. All key parameters are summarized in Table 3.

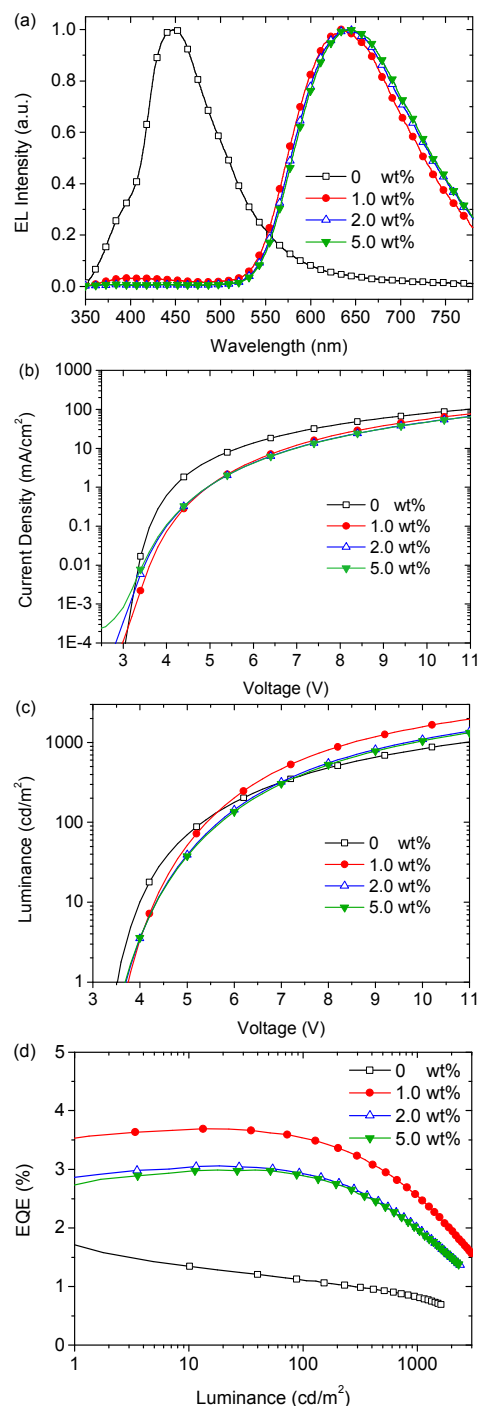
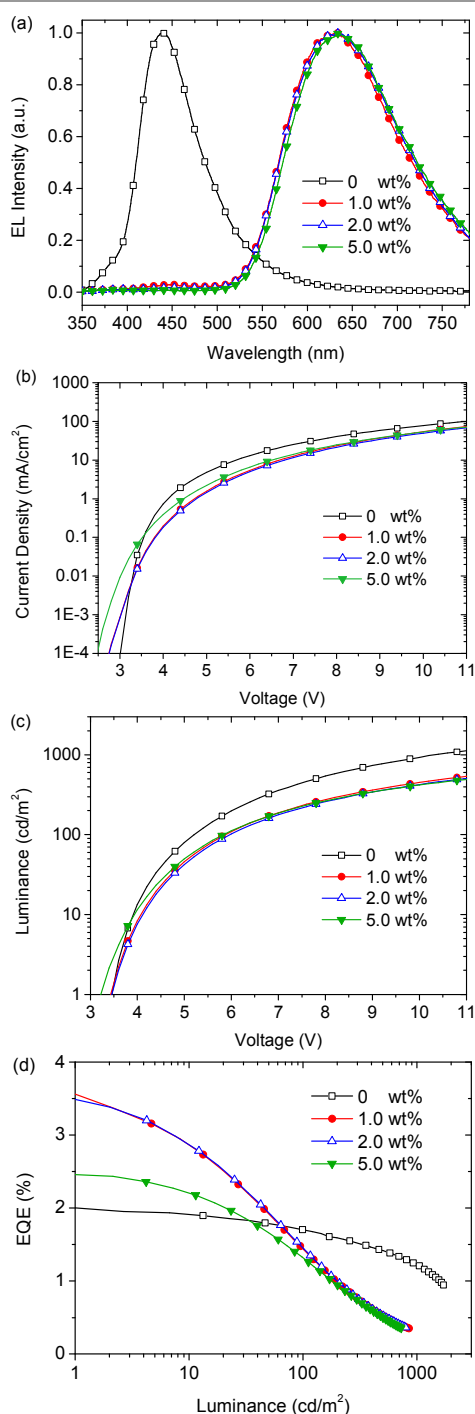


Fig. 7. (a) EL spectra, (b) CD-V, (c) L-V, and (d) EQE-L characteristics of devices 1-4 with configuration of  $\text{ITO}/\text{MoO}_3$  (1 nm)/  $\text{CBP}$  (35 nm)/  $\text{CuI}:\text{DCIQ}$  ( $x \text{ wt\%}$ , 20 nm)/  $\text{TPBi}$  (65 nm)/  $\text{LiF}$  (1 nm)/  $\text{Al}$ , where  $x = 0$  (device 1), 1.0 (device 2), 2.0 (device 3), and 5.0 (device 4), respectively.



**Fig. 8.** (a) EL spectra, (b) CD-V, (c) L-V, and (d) EQE-L characteristics of devices 5-8 with configuration of ITO/ MoO<sub>3</sub> (1 nm)/ CBP (35 nm)/ CuI:DCDPIQ (*x* wt%, 20 nm)/ TPBi (65 nm)/ LiF (1 nm)/ Al, where *x* = 0 (device 5), 1.0 (device 6), 2.0 (device 7), and 5.0 (device 8), respectively.

As shown in Fig. 7a and 8a, the devices 1 and 5 without CuI showed blue emission with CIE of (0.17, 0.16) and (0.17, 0.13) that arise from neat DCIQ and DCDPIQ film, respectively. The devices 2-4 and 6-8 showed significantly different emission from those of device 1 and 5, with maximum EL bands around 643 and 635 nm, indicating that the luminescence arise from a CuI:DCIQ and CuI:DCDPIQ complex, respectively, which is in

consistent with the aforementioned PL study. EL solely from CuI:DCIQ and CuI:DCDPIQ were observed in devices 3-4 and 7-8 under all applied currents (Fig. S5). Devices 2 and 6, with higher DCIQ and DCDPIQ concentrations (i.e. lower CuI doping concentration and consequently lower Cu<sup>I</sup> complex doping concentration), exhibited a very small emissive contribution from DCIQ and DCDPIQ at high current densities, respectively. This is expected as a higher Cu<sup>I</sup> complex doping concentration would lead to a complete energy transfer from CIQ to its *in situ* synthesized Cu<sup>I</sup> complex.

Due to high PLQYs in neat film, the blue devices 1 and 5 using DCIQ and DCDPIQ film as the EML showed good performance. For example, the device 1 with DCIQ EML showed a turn-on voltage ( $V_{on}$ ) of 3.5 V, maximum luminance ( $L_{max}$ ) of 1632 cd m<sup>-2</sup> (15 V), maximum power efficiency ( $PE_{max}$ ) and current efficiency ( $CE_{max}$ ) of 1.9 lm W<sup>-1</sup> and 2.1 cd A<sup>-1</sup>, respectively, corresponding to a maximum EQE of 1.7 %. The device 2 showed a  $V_{on}$ ,  $L_{max}$ ,  $PE_{max}$ ,  $CE_{max}$ , and  $EQE_{max}$  of 3.4 V, 1743 cd m<sup>-2</sup> (15 V), 1.7 lm W<sup>-1</sup>, 1.9 cd A<sup>-1</sup>, and 2.0%, respectively (Table 3). These results may provide insights into the strategies of designing novel blue emitting compounds for the fabrication of high efficiency OLEDs.

All the codeposited OLEDs showed device performance scaling with CuI doping concentrations. For example, the best performance was observed in the devices 2 and 6, for DCIQ and DCDPIQ, respectively, with an optimal CuI doping concentration of 1.0 wt%. It should be noted that the CuI:DCDPIQ devices 6-8 drop quickly in EQE as compared to the non-doped device 5 when increasing the luminance of the devices (Fig. 8d). This may be attributed to an unbalanced charge recombination in the CuI-doped device at high luminance (i.e. high current density), since the doping of CuI changes not only the photophysical property of the emissive layer, but also its electrical property. To further summarize the performance of these OLEDs (Table 3), the best OLED was obtained with a CuI:DCDPIQ EML, having peak PE, CE and EQE of 4.8 lm W<sup>-1</sup>, 5.2 cd A<sup>-1</sup> and 3.6%, respectively. While the most saturated red emissive OLED was achieved using DCIQ as the ligand/host material and a CuI doping concentration of 5 wt%, showing maximum PE, CE and EQE of 2.7 lm W<sup>-1</sup>, 3.1 cd A<sup>-1</sup> and 2.7%, respectively. At a brightness of 100 cd m<sup>-2</sup>, a PE of 1.8 lm W<sup>-1</sup> with an EQE of 2.9% ( $CE = 3.3$  cd A<sup>-1</sup>) was obtained. To our best of knowledge, the performance is among the best red emitting OLEDs that using Cu<sup>I</sup> complex as the emitter.<sup>24, 28, 35</sup>

## Conclusions

In summary, two isoquinolyl carbazole (CIQ) compounds were designed and synthesized to *in situ* codeposition with CuI to form Cu<sup>I</sup> complex doped emissive films, which could be used as EML in OLEDs. Since the compound serves a dual role as both a ligand for forming the emissive complex and as a host matrix for the formed emitter, a systematical study was conducted both on these compounds and their codeposited CuI:CIQ films, including photophysical properties,

electrochemical properties, and thermostability. Furthermore, the two compounds were evaluated in OLEDs with a device structure of ITO/ MoO<sub>3</sub> (1 nm)/ CBP (35 nm)/ CuI:DCIQ or DCDPIQ (20 nm)/ TPBi (65 nm)/ LiF (1 nm)/ Al. By optimizing CuI doping concentration, the DCIQ based OLEDs showed maximum emission band, EQE, and luminance of 643 nm, 3.5%, and 3290 cd m<sup>-2</sup> respectively, while the DCDPIQ based OLEDs showed those of 635 nm, 3.6%, and 853 cd m<sup>-2</sup> respectively. The results demonstrated here implies that the emission color of the *in situ* synthesized Cu<sup>I</sup> complex can be tuned as well as colorful OLEDs fabricated with inexpensive and eco-friendly Cu<sup>I</sup> complexes.

## Experimental

### General information

<sup>1</sup>H and <sup>13</sup>C-NMR spectra were recorded on a Varian-400 and Bruker-500 MHz spectrometer, respectively. Chemical shifts were reported in ppm relative to the singlet of CDCl<sub>3</sub> at 7.26 and 77 ppm for <sup>1</sup>H and <sup>13</sup>C NMR, respectively. Mass spectra were measured on a Bruker Apex IV FTMS. Elemental analyses were performed on a VARIO EL analyzer (GmbH, Hanau, Germany).

### Photophysical Measurement

UV-vis absorption spectra were recorded on a Shimadzu UV-3100 spectrometer. PL spectra at room temperature were measured on an Edinburgh Analytical Instruments FLS920 spectrophotometer, while those at 77 K were measured on Hitachi fluorescence spectrophotometer F-7000 with a fluorescence and phosphorescence model. PLQYs were measured on Quantaurus-QY C11347-11 absolute PLQYs measurement system.

### Theoretical Calculations

For calculation of HOMO and LUMO energy levels, ground states (S<sub>0</sub>) and triplet excited states (T<sub>1</sub> and T<sub>2</sub>), DFT calculations were performed for optimized molecular structures and single-point energies at the B3LYP/6-31G(d) and B3LYP/6-311+G(d, p) levels, respectively, using a Gaussian suite of programs (Gaussian 03W).<sup>48</sup>

### Thermal Properties Measurements

Thermogravimetric analysis was undertaken with a Q100DSC instrument. The thermal stability of the samples under a nitrogen atmosphere was determined by measuring their weight loss while heating at a rate of 15 °C min<sup>-1</sup> from 25 to 600 °C. Differential scanning calorimetry was performed on a Q600SDT instrument unit at a heating rate of 15 °C min<sup>-1</sup> from 20 to 300 °C under nitrogen. The glass transition temperature was determined from the second or the third heating scan.

### Cyclic Voltammetry Measurements

Cyclic voltammetry was carried out in nitrogen-purged CH<sub>2</sub>Cl<sub>2</sub> solution at room temperature with a CHI600C voltammetric

analyzer and tetrabutylammonium hexafluorophosphate (TBAPF<sub>6</sub>) (0.1 M) as the supporting electrolyte. The conventional three-electrode configuration consists of a platinum working electrode, a platinum wire auxiliary electrode, and an Ag/AgCl wire pseudo-reference electrode.

### X-ray Absorption Fine-Structure Measurements

The X-ray absorption data at the Cu *K*-edge of codeposited CuI:DCDPIQ film was measured at room temperature in fluorescence mode with an SDD detector at beam line BL14W of the Shanghai Synchrotron Radiation Facility (SSRF), China.

### OLED Fabrication and Measurements

The indium-tin oxide (ITO)-coated glass, hole injection material MoO<sub>3</sub>, hole transporting material CBP, electron transporting material TPBi, and electron injection material LiF/Al were commercially available. In a general procedure, ITO-coated glass substrate was deposited with MoO<sub>3</sub> (1 nm) and then treated by *ex situ* UV ozone for 7 min. Then the substrate was transferred to the deposition system. CBP (35 nm) was firstly deposited onto ITO/MoO<sub>3</sub> substrate, followed by emissive layer (20 nm), and TPBi (65 nm). Finally, a cathode composed of LiF (1 nm) and Al (100 nm) was sequentially deposited onto the substrate in another vacuum chamber (10<sup>-5</sup> Pa). The luminance-current density-voltage (L-I-V) was measured using a HP4140B picoammeter and Minolta LS-110 luminance meter. The EL spectra were recorded using an USB2000-UV-vis Miniature Fiber Optic Spectrometer. All measurements were carried out in ambient atmosphere and at room temperature.

### Syntheses of DCIQ and DCDPIQ

**5,8-dibromoisoquinoline (1)**<sup>39</sup>: To mechanically stirred H<sub>2</sub>SO<sub>4</sub> (70 mL) at -25 °C was added isoquinoline (8.0 mL, 68 mmol). Then NBS (28.01 g, 157 mmol) was added slowly while keeping the temperature between -25 to -20 °C. The mixture was stirred at this temperature and room temperature for 1 h, respectively. After that, the mixture was poured into iced-water (350 mL) and the pH was adjusted to 8 by aqueous NH<sub>3</sub>. The precipitate was filtered off, air-dried, and purified by column chromatography. Further recrystallization by methanol/CH<sub>2</sub>Cl<sub>2</sub> was obtained 13.10 g white powder (yield: 67%). <sup>1</sup>H-NMR (400 MHz, CDCl<sub>3</sub>, δ): 9.70 (s, 1 H), 8.73 (d, *J* = 6.4 Hz, 1 H), 8.25 (d, *J* = 6.0 Hz, 1 H), 7.99 (d, *J* = 8.4 Hz, 1 H), 7.86 (d, *J* = 8.0 Hz, 1 H); MS: expected *m/z* = 287.9, found *m/z* = 287.9.

**4-(carbazol-9-yl)phenylboronic acid (2)**: To a solution of 9-(4-bromophenyl)-carbazole (7.72 g, 24.0 mmol) in THF (150 mL) at -78 °C was added slowly n-BuLi (12 mL, 2.4 M in hexane). After stirred for 1 h, trimethyl borate (4.8 mL, 36 mmol) was added. The mixture was then stirred for another 2 h and allowed to warm to room temperature slowly and stirred overnight, then 20 mL hydrochloric acid (2 M) was added to adjust the pH = 5. After extraction and recrystallization in CH<sub>2</sub>Cl<sub>2</sub>, 4.76 g (yield: 70%) white product was obtained. <sup>1</sup>H-

NMR (400 MHz, DMSO- $d_6$ ,  $\delta$ ): 8.27 (m, 4 H), 7.68 (d,  $J = 6.4$  Hz, 2 H), 7.44 (m, 4 H), 7.30 (t,  $J = 8.0$  Hz, 2 H).

**9-(8-(carbazol-9-yl)isoquinolin-5-yl)-carbazole (DCIQ):** Compound 1 (1.75 g, 6.10 mmol), carbazole (2.27 g, 13.6 mmol),  $K_2CO_3$  (2.45 g, 17.7 mmol), and Cu (0.80 g, 12 mmol) were added into nitrobenzene (27 mL). The mixture was refluxed with  $N_2$  protection for 24 h. After cooling to room temperature, the reaction mixture was filtered and the residue was washed with  $CH_2Cl_2$ . The solvent of the filtrate was removed by distillation at a reduced pressure. The residue was purified by column chromatography to obtain 1.54 g solid (yield: 56%). Further purification was conducted by sublimation twice under a temperature gradient of 250 °C -180 °C -100 °C.  $^1H$ -NMR (400 MHz,  $CDCl_3$ ,  $\delta$ ): 9.03 (s, 1 H), 8.48 (s, 1 H), 8.26 (d,  $J = 7.2$  Hz, 4 H), 8.20 (d,  $J = 8.0$  Hz, 1 H), 8.04 (d,  $J = 8.0$  Hz, 1H), 7.43 (m, 9H), 7.15 (t,  $J = 8.0$  Hz, 4H);  $^{13}C$ -NMR (500 MHz,  $CDCl_3$ ,  $\delta$ ): 149.70-148.68 (m), 142.19 (s), 141.83 (s), 136.05-135.68 (m), 135.36-135.10 (m), 134.09 (s), 131.97-131.09 (m), 128.24 (s), 126.46 (s), 126.37 (s), 123.80 (s), 123.71 (s), 120.77 (s), 120.71-120.42 (m), 109.95 (s), 109.92 (s); MS: expected  $m/z = 460.2$ , found  $m/z = 460.2$ ; Anal. Calcd. for  $C_{33}H_{21}N_3$ : C, 86.25; H, 4.61; N, 9.14. Found: C, 86.11; H, 4.54; N, 9.12.

**9-(4-(5-(4-(carbazol-9-yl)phenyl)isoquinolin-8-yl)phenyl)-carbazole (DCDPIQ):** Compounds 1 (0.75 g, 2.6 mmol), 2 (1.65 g, 5.75 mmol) and  $Pd(PPh_3)_4$  (0.275 g, 0.238 mmol) were added into a mixed solvent of 75 mL toluene, 35 mL ethanol and 35 mL 2 M  $K_2CO_3$ . Under  $N_2$  protection, the mixture was refluxed at 90 °C for 24 h. After extraction with  $CH_2Cl_2$ , the crude product was purified by column chromatography and yielded 1.10 g product (yield: 69%). Further purification was conducted by sublimation twice under a gradient temperature of 300 °C -220 °C -120 °C.  $^1H$ -NMR (400 MHz,  $CDCl_3$ ,  $\delta$ ): 9.59 (s, 1H), 8.65 (d,  $J = 6.0$  Hz, 1 H), 8.20 (d,  $J = 7.6$  Hz, 4 H), 8.08 (d,  $J = 6.0$  Hz, 1 H), 7.96 (d,  $J = 7.6$  Hz, 1H), 7.83 (m, 9 H), 7.60 (d,  $J = 8.0$  Hz, 4 H), 7.50 (t,  $J = 7.6$  Hz, 4 H), 7.35 (t,  $J = 7.6$  Hz, 4 H);  $^{13}C$ -NMR (500 MHz,  $CDCl_3$ ,  $\delta$ ): 151.78-150.58 (m), 144.38-142.54 (m), 140.84 (s), 140.33-139.50 (m), 138.15 (s), 137.99 (s), 137.81 (s), 137.65 (s), 137.62-137.57 (m), 134.72 (s), 131.64 (s), 131.44 (s), 130.80 (s), 128.06 (s), 127.20 (s), 127.18 (s), 127.01 (s), 126.12 (s), 126.09 (s), 123.62 (s), 120.45 (s), 120.43-120.41 (m), 120.23 (s), 118.67 (s), 109.86 (s), 109.83 (s); MS: expected  $m/z = 612.2$ , found  $m/z = 612.2$ ; Anal. Calcd. for  $C_{45}H_{29}N_3$ : C, 88.35; H, 4.78; N, 6.87. Found: C, 88.22; H, 4.80; N, 6.88.

## Acknowledgements

We greatly acknowledge the financial support by The National Basic Research Program of China (No. 2014CB643802), The National Natural Science Foundation of China (NNSFC, Nos. 21201011, 21371012, 91127001), and The Specialized Research Fund for the Doctoral Program of Higher Education (20120001120116).

## Notes and references

<sup>a</sup> Beijing National Laboratory for Molecular Sciences (BNLMS), State Key Laboratory of Rare Earth Materials Chemistry and Applications, College of Chemistry and Molecular Engineering, Peking University, Beijing 100871, P. R. China. E-mail: zwliu@pku.edu.cn, Fax: (+86) 10-6275-3544, Tel: (+86) 10-6275-7156.

<sup>b</sup> Department of Physics, Yunnan University, 2 Cuihu Bei Lu, Kunming, 650091, P. R. China.

<sup>c</sup> Key Laboratory of Interfacial Physics and Technology, Shanghai Institute of Applied Physics, Chinese Academy of Sciences, Shanghai 201204, P. R. China. Email: wangjianqiang@sinap.ac.cn

† Electronic Supplementary Information (ESI) available: DFT calculation, PL spectra in solid state at room temperature and 77 K, thermogravimetric analysis of DCIQ and DCDPIQ, photophysical properties of codeposited CuI:CIQ films with different CuI:CIQ molar ratios, experimental data and calculated data for Cu  $K$ -edge XANES of the codeposited CuI:DCDPIQ film with different local structure models, EL spectra of all OLEDs at different currents. See DOI: 10.1039/b000000x/

- H. Sasabe, J. Kido, *Chem. Mater.*, 2011, **23**, 621.
- C. Perez-Bolivar, S. Y. Takizawa, G. Nishimura, V. A. Montes, P. Anzenbacher, *Chem. Eur. J.*, 2011, **17**, 9076.
- G. J. Zhou, X. L. Yang, W. Y. Wong, Q. Wang, S. Suo, D. G. Ma, J. K. Feng, L. X. Wang, *ChemPhysChem*, 2011, **12**, 2836.
- T. Hu, L. He, L. Duan, Y. Qiu, *J. Mater. Chem.*, 2012, **22**, 4206.
- A. Kohnen, M. Irion, M. C. Gather, N. Rehmman, P. Zacharias, K. Meerholz, *J. Mater. Chem.*, 2010, **20**, 3301.
- J. N. Yu, H. Lin, F. F. Wang, Y. Lin, J. H. Zhang, H. Zhang, Z. X. Wang, B. Wei, *J. Mater. Chem.*, 2012, **22**, 22097.
- S. Reineke, F. Lindner, G. Schwartz, N. Seidler, K. Walzer, B. Lussem, K. Leo, *Nature*, 2009, **459**, 234.
- M. H. Li, W. H. Chen, M. T. Lin, M. A. Omary, N. D. Shepherd, *Org Electron.*, 2009, **10**, 863.
- Y. H. Xu, J. B. Peng, Y. Cao, *Prog. Chem.*, 2006, **18**, 389.
- M. A. Baldo, D. F. O'Brien, Y. You, A. Shoustikov, S. Sibley, M. E. Thompson, S. R. Forrest, *Nature*, 1998, **395**, 151.
- Y. R. Sun, N. C. Giebink, H. Kanno, B. W. Ma, M. E. Thompson, S. R. Forrest, *Nature*, 2006, **440**, 908.
- S. Lamansky, P. Djurovich, D. Murphy, F. Abdel-Razzaq, H. E. Lee, C. Adachi, P. E. Burrows, S. R. Forrest, M. E. Thompson, *J. Am. Chem. Soc.*, 2001, **123**, 4304.
- J. A. G. Williams, S. Develay, D. L. Rochester, L. Murphy, *Coord. Chem. Rev.*, 2008, **252**, 2596.
- Y. Chi, P. T. Chou, *Chem. Soc. Rev.*, 2010, **39**, 638.
- Z. B. Wang, M. G. Helander, J. Qiu, D. P. Puzzo, M. T. Greiner, Z. M. Hudson, S. Wang, Z. W. Liu, Z. H. Lu, *Nat. Photonics*, 2011, **5**, 753.
- M. G. Helander, Z. B. Wang, J. Qiu, M. T. Greiner, D. P. Puzzo, Z. W. Liu, Z. H. Lu, *Science*, 2011, **332**, 944.
- H. Uoyama, K. Goushi, K. Shizu, H. Nomura, C. Adachi, *Nature*, 2012, **492**, 234.
- P. C. Ford, E. Cariati, J. Bourassa, *Chem. Rev.*, 1999, **99**, 3625.
- N. Armadori, G. Accorsi, F. Cardinali, A. Listorti, *Top. Curr. Chem.*, 2007, **280**, 69.
- R. C. Evans, P. Douglas, C. J. Winscom, *Coord. Chem. Rev.*, 2006, **250**, 2093.
- Y. G. Ma, W. H. Chan, X. M. Zhou, C. M. Che, *New J. Chem.*, 1999, **23**, 263.
- Y. G. Ma, C. M. Che, H. Y. Chao, X. M. Zhou, W. H. Chan, J. C. Shen, *Adv. Mater.*, 1999, **11**, 852.
- Q. S. Zhang, Q. G. Zhou, Y. X. Cheng, L. X. Wang, D. G. Ma, X. B. Jing, F. S. Wang, *Adv. Mater.*, 2004, **16**, 432.
- G. B. Che, Z. S. Su, W. L. Li, B. Chu, M. T. Li, Z. Z. Hu, Z. Q. Zhang, *Appl. Phys. Lett.*, 2006, **89**, 103511.

- 25 Q. S. Zhang, Q. G. Zhou, Y. X. Cheng, L. X. Wang, D. G. Ma, X. B. Jing, F. S. Wang, *Adv. Funct. Mater.*, 2006, **16**, 1203.
- 26 A. Tsuboyama, K. Kuge, M. Furugori, S. Okada, M. Hoshino, K. Ueno, *Inorg. Chem.*, 2007, **46**, 1992.
- 27 L. M. Zhang, B. Li, Z. M. Su, *J. Phys. Chem. C*, 2009, **113**, 13968.
- 28 J. C. Deaton, S. C. Switalski, D. Y. Kondakov, R. H. Young, T. D. Pawlik, D. J. Giesen, S. B. Harkins, A. J. M. Miller, S. F. Mickenberg, J. C. Peters, *J. Am. Chem. Soc.*, 2010, **132**, 9499.
- 29 M. Hashimoto, S. Igawa, M. Yashima, I. Kawata, M. Hoshino, M. Osawa, *J. Am. Chem. Soc.*, 2011, **133**, 10348.
- 30 Z. W. Liu, M. F. Qayyum, C. Wu, M. T. Whited, P. I. Djurovich, K. O. Hodgson, B. Hedman, E. I. Solomon, M. E. Thompson, *J. Am. Chem. Soc.*, 2011, **133**, 3700.
- 31 Q. S. Zhang, T. Komino, S. P. Huang, S. Matsunami, K. Goushi, C. Adachi, *Adv. Funct. Mater.*, 2012, **22**, 2327.
- 32 X. L. Chen, R. M. Yu, Q. K. Zhang, L. J. Zhou, C. Y. Wu, Q. Zhang, C. Z. Lu, *Chem. Mater.*, 2013, **25**, 3910.
- 33 M. Osawa, I. Kawata, R. Ishii, S. Igawa, M. Hashimoto, M. Hoshino, *J. Mater. Chem. C*, 2013, **1**, 4375.
- 34 Sun, Q. S. Zhang, L. Qin, Y. X. Cheng, Z. Y. Xie, C. Z. Lu, L. X. Wang, *Eur. J. Inorg. Chem.*, 2010, **25**, 4009.
- 35 H. Ge, W. Wei, P. Shuai, G. Lei, S. Qing, *J. Lumin.*, 2011, **131**, 238.
- 36 Z. W. Liu, J. Qiu, F. Wei, J. Q. Wang, X. C. Liu, M. G. Helander, S. Rodney, Z. B. Wang, Z. Q. Bian, Z. H. Lu, M. E. Thompson, C. H. Huang, *Chem. Mater.*, 2014, **26**, 2368.
- 37 D. M. Zink, M. Bachle, T. Baumann, M. Nieger, M. Kuhn, C. Wang, W. Klopper, U. Monkowius, T. Hofbeck, H. Yersin, S. Brase, *Inorg. Chem.*, 2013, **52**, 2292.
- 38 H. Araki, K. Tsuge, Y. Sasaki, S. Ishizaka, N. Kitamura, *Inorg. Chem.*, 2005, **44**, 9667.
- 39 W. D. Brown, A. H. Goulliaev, *Synthesis*, 2002, **1**, 83.
- 40 K. Y. Wang, C. Chen, J. F. Liu, Q. Wang, J. Chang, H. J. Zhu, C. Li, *Org. Biomol. Chem.*, 2012, **10**, 6693.
- 41 M. H. Tsai, Y. H. Hong, C. H. Chang, H. C. Su, C. C. Wu, A. Matoliukstyte, J. Simokaitiene, S. Grigalevicius, J. V. Grazulevicius, C. P. Hsu, *Adv. Mater.*, 2007, **19**, 862.
- 42 J. N. Moorthy, P. Venkatakrishnan, D. F. Huang, T. J. Chow, *Chem. Commun.*, 2008, **18**, 2146.
- 43 X. Zhou, J. He, L. S. Liao, M. Lu, X. M. Ding, X. Y. Hou, X. M. Zhang, X. Q. He, S. T. Lee, *Adv. Mater.*, 2000, **12**, 265.
- 44 B. W. D'Andrade, S. Datta, S. R. Forrest, P. I. Djurovich, E. Polikarpov, M. E. Thompson, *Org. Electron.*, 2005, **6**, 11.
- 45 F. Wei, J. Qiu, X. C. Liu, J. Q. Wang, H. B. Wei, Z. B. Wang, Z. W. Liu, Z. Q. Bian, Z. H. Lu, Y. L. Zhao, C. H. Huang, *J. Mater. Chem. C*, 2014, **2**, 6333.
- 46 A. L. Ankudinov, B. Ravel, J. J. Rehr, S. D. Conradson, *Phys. Rev. B*, 1998, **58**, 7565.
- 47 M. A. Baldo, S. R. Forrest, *Phys. Rev. B*, 2000, **62**, 10958.
- 48 M. J. Frisch, G. W. Trucks, H. B. Schlegel, G. E. Scuseria, M. A. Robb, J. R. Cheeseman, J. A. Jr. Montgomery, T. Vreven, K. N. Kudin, J. C. Burant, J. M. Millam, S. S. Iyengar, J. Tomasi, V. Barone, B. Mennucci, M. Cossi, G. Scalmani, N. Rega, G. A. Petersson, H. Nakatsuji, M. Hada, M. Ehara, K. Toyota, R. Fukuda, J. Hasegawa, M. Ishida, T. Nakajima, Y. Honda, O. Kitao, H. Nakai, M. Klene, X. Li, J. E. Knox, H. P. Hratchian, J. B. Cross, V. Bakken, C. Adamo, J. Jaramillo, R. Gomperts, R. E. Stratmann, O. Yazyev, A. J. Austin, R. Cammi, C. Pomelli, J. W. Ochterski, P. Y. Ayala, K. Morokuma, G. A. Voth, P. Salvador, J. J. Dannenberg, V. G. Zakrzewski, S. Dapprich, A. D. Daniels, M. C. Strain, O. Farkas, D. K. Malick, A. D. Rabuck, K. Raghavachari, J. B. Foresman, J. V. Ortiz, Q. Cui, A. G. Baboul, S. Clifford, J. Cioslowski, B. B. Stefanov, G. Liu, A. Liashenko, P. Piskorz, I. Komaromi, R. L. Martin, D. J. Fox, T. Keith, M. A. Al-Laham, C. Y. Peng, A. Nanayakkara, M. Challacombe, P. M. W. Gill, B. Johnson, W. Chen, M. W. Wong, C. Gonzalez, J. A. Pople, *Gaussian 03*, revision B.04; Gaussian, Inc.: Wallingford, CT, 2003.

Red emissive  $\text{Cu}^{\text{I}}$  complexes and their organic light-emitting diodes were prepared by codeposition of  $\text{CuI}$  and isoquinoline based ligands.

